

UNCLASSIFIED

AD 429850

DEFENSE DOCUMENTATION CENTER

FOR

SCIENTIFIC AND TECHNICAL INFORMATION

CAMERON STATION, ALEXANDRIA, VIRGINIA



UNCLASSIFIED

NOTICE: When government or other drawings, specifications or other data are used for any purpose other than in connection with a definitely related government procurement operation, the U. S. Government thereby incurs no responsibility, nor any obligation whatsoever; and the fact that the Government may have formulated, furnished, or in any way supplied the said drawings, specifications, or other data is not to be regarded by implication or otherwise as in any manner licensing the holder or any other person or corporation, or conveying any rights or permission to manufacture, use or sell any patented invention that may in any way be related thereto.

4 298 50

CATALOGED BY DDC

AS AD No. _____

429850

64 7

COLLAPSE, BUCKLING AND POST FAILURE
OF CYLINDRICAL SHELLS

Joshua E. Greenspon, Dr. Eng.

Contract No. DA 36-034-ORD-3081 RD
Technical Report No. 4
December, 1963

J G ENGINEERING RESEARCH ASSOCIATES
3831 MENLO DRIVE BALTIMORE 15, MARYLAND

COLLAPSE, BUCKLING AND POST FAILURE
OF CYLINDRICAL SHELLS

Joshua E. Greenspon, Dr. Eng.
J G ENGINEERING RESEARCH ASSOCIATES
3831 Menlo Drive
Baltimore, Maryland 21215

Ballistic Research Laboratories
Aberdeen Proving Ground
Contract No. DA 36-034-ORD-3081 RD
Technical Report No. 4
December, 1963

(Reproduction in whole or in part is permitted for
any purpose of the United States Government)

ABSTRACT

In this report it is demonstrated how simple existing theories can predict whether a shell will fail by buckling or form a collapse hinge and then fail by this collapse mechanism. It is also shown how work-energy analysis can predict the post failure plastic deflections of the shell once the mode of failure is known. Some comparisons with experimental results are given.

TABLE OF CONTENTS

	Page
I. Introduction	1
II. Elastic Stress Analysis	1
III. Elastic Buckling Analysis	3
IV. Buckling or Yield	3
V. Post Failure Collapse and Buckling	5
A. Collapse	
B. Buckling	
VI. Conclusions	9
References	10
Figures	11

ACKNOWLEDGEMENTS

This work was done under the sponsorship of Ballistic Research Laboratories at Aberdeen Proving Ground. The technical supervisor of the project is Mr. William Schuman. The author is grateful to Mr. Schuman for many valuable suggestions and is grateful to Ballistic Research Laboratories for their continued support.

LIST OF SYMBOLS

$N_\phi, N_{x\phi}, N_x$	stress resultants
x	longitudinal coordinate
ϕ	peripheral coordinate
$f_1(\phi), f_2(\phi)$ $f_3(\phi), f_4(\phi)$	arbitrary functions of ϕ which are determined from the boundary conditions
a	mean radius of the shell
$p(x, \phi)$	pressure distribution
h	thickness of shell
u, v, w	longitudinal, tangential and radial displacements respectively
α, β	parameters used to define the peripheral pressure amplitude
ν	Poisson's ratio
E	modulus of elasticity
l	length of shell
n	number of circumferential waves in buckling pattern
σ_0	yield stress in pure tension
$(p_0)_c$	pressure which initiates collapse
$(p_{cr})_b$	pressure which initiates buckling
ρ	mass density of shell material
$g(x, y)$	spatial distribution of the impulse
V	work done by shell in deforming
w_0	maximum deflection amplitude
$F(x, \phi)$	spatial distribution of the deflection
ϵ_0	yield strain in pure tension
x'	x/l
d_0	width of plastic hinge
K	defined by Eq. [20]
I_t	total impulse (theoretical)
\bar{I}	defined by Eq. [22]
\bar{I}_e	experimental impulse per unit area
$(\bar{I}_e)_r$	reflected experimental impulse per unit area
$(\bar{I}_e)_i$	incident experimental impulse per unit area
k	parameter defining periphery die out of spatial deflection distribution in buckling

I. Introduction

A previous report^{1*} presented the plastic work expressions for cylindrical shells and discussed the types of failure that could occur in cylindrical shells under blast loading. Experiments have shown² that cylindrical shells subjected to side-on blast can go into two main types of failure. These are buckling and collapse. The buckling type of failure is described by a deformation pattern which consists of a number of lobes around the periphery of the shell and one half wave length along the length as shown in Figure 1a. The collapse failure is described by a straight failure hinge at the center of the shell as shown in Figure 1b. Both of these figures are taken from Schuman's experimental results.² The type of failure will depend upon the geometry of the shell and can be predicted from an elastic stress and buckling analysis of the shell as will be seen later in this report.

II. Elastic stress analysis

Assume that the shell is thin and that membrane theory is adequate to describe the stress patterns in the shell. Assume also that the shell is of length l and is supported at each end. Take the origin of coordinates at the center of the shell as shown in Figure 2. The membrane forces are shown on the differential element in Figure 3.

If $p(x, \varphi)$ is the static load per unit area applied laterally to the shell then it follows from the basic membrane equations^{3,4} that

$$\begin{aligned} N_{\varphi} &= a p(x, \varphi) \\ N_{x\varphi} &= - \int \frac{1}{a} \frac{\partial N_{\varphi}}{\partial \varphi} dx + f_1(\varphi) \\ N_x &= - \int \frac{1}{a} \frac{\partial N_{x\varphi}}{\partial \varphi} dx + f_2(\varphi) \end{aligned} \quad [1]$$

where $f_1(\varphi)$ and $f_2(\varphi)$ are functions of φ which are to be determined from the boundary conditions on $N_x, N_{x\varphi}, N_{\varphi}$. If some of the boundary conditions are given in terms of displacements then the following membrane equations in terms of displacements must be utilized³

*Superscripts refer to references given at the back of the report.

$$\begin{aligned}
Eh u &= \int (N_x - \nu N_\varphi) dx + f_3(\varphi) \\
Eh v &= 2(1+\nu) \int N_{x\varphi} dx - \frac{Eh}{a} \int \frac{\partial u}{\partial \varphi} dx + f_4(\varphi) \\
Eh w &= a(N_\varphi - \nu N_x) + Eh \frac{\partial v}{\partial \varphi}
\end{aligned} \tag{2}$$

where h is the shell thickness, E is the modulus of elasticity, u, v, w are the displacements (see Fig. 3) and $f_3(\varphi), f_4(\varphi)$ are arbitrary functions to be determined from the boundary conditions.

Now assume that the pressure $p(x, \varphi)$ can be represented as

$$\begin{aligned}
p(x, \varphi) &= p_0 e^{-\beta \varphi} \cos \alpha \varphi \quad 0 < \varphi < \pi \\
&= p_0 e^{-\beta(2\pi - \varphi)} \cos \alpha(2\pi - \varphi) \quad \pi < \varphi < 2\pi
\end{aligned} \tag{3}$$

where p_0 is the maximum amplitude of the pressure and β, α are parameters determining the peripheral pressure distribution. If the shell length is small compared to the distance from the explosion and if the blast is a side-on load then it seems reasonable that the spatial load distribution given by [3] should resemble the spatial distribution produced by the blast.

The solution will be obtained for the boundary conditions

$$\begin{aligned}
u &= 0 \quad \text{at} \quad x = \pm l/2 \\
(N_{x\varphi} &= 0 \quad \text{at} \quad x = 0 \quad \text{by symmetry})
\end{aligned} \tag{4}$$

By straight forward integration of equations [1] and [2] subject to boundary conditions [4] it is found that

$$\begin{aligned}
N_\varphi &= a p_0 f(\varphi), \quad f(\varphi) = e^{-\beta \varphi} \cos \alpha \varphi \\
N_{x\varphi} &= -p_0 x \quad f'(\varphi) = \frac{df}{d\varphi}, \quad f''(\varphi) = \frac{d^2 f}{d\varphi^2} \\
N_x &= \frac{p_0}{a} \frac{x^2}{2} f''(\varphi) + \nu a p_0 f(\varphi) - \frac{p_0}{a} \frac{l^2}{24} f''(\varphi)
\end{aligned} \tag{5}$$

The stress resultants at $x = \varphi = 0$ are

$$\begin{aligned}
N_\varphi &= a p_0 \\
N_{x\varphi} &= 0 \\
N_x &= \nu a p_0 - \frac{p_0}{a} \frac{l^2}{24} (\beta^2 - \alpha^2)
\end{aligned} \tag{6}$$

Yielding will occur at $x = \varphi = 0$ when the Von Mises Yield Condition is satisfied at this point, i.e.

$$N_x^2 - N_x N_\varphi + N_\varphi^2 + 3 N_{x\varphi}^2 = \sigma_0^2 h^2 \tag{7}$$

where σ_0 is the yield stress in pure tension. Substituting the values of the stress resultants into the yield condition it is found that yielding will occur at the center of the shell ($\alpha = 0, \phi = 0$) when the pressure p_0 has a value

$$(p_0)_c = \sigma_0 \frac{h}{a} \frac{1}{\sqrt{(1-\nu+\nu^2) + (\beta^2 - \alpha^2) \left[\frac{\ell^2}{24a^2} (1-2\nu) + \left(\frac{\ell^2}{24a^2} \right)^2 (\beta^2 - \alpha^2) \right]}} \quad [8]$$

III. Elastic buckling analysis

The classical theory of buckling of cylindrical shells is presented by Timoshenko.⁵ It is found that the lateral pressure at which buckling under uniform loading will occur is given by the following relation⁶

$$(q_{cr})_b = \frac{Eh}{a(1-\nu^2)} \left[\frac{1-\nu^2}{(n^2-1) \left(1 + \frac{n^2 \ell^2}{\pi^2 a^2} \right)^2} + \frac{h^2}{12a^2} \left(n^2 - 1 + \frac{2n^2 - 1 - \nu}{1 + \frac{n^2 \ell^2}{\pi^2 a^2}} \right) \right] \quad [9]$$

where n is the number of full waves around the periphery of the shell. It has been found by Reynolds⁷ that in lobar buckling such as this the circumferential parameter n approximately satisfies the relation

$$\frac{1}{1 + \frac{n^2 \ell^2}{\pi^2 a^2}} \approx 1.23 \frac{\sqrt{ah}}{\ell} \quad [10]$$

and that buckling will always occur with only one half wave along the length. In other words, if m denotes the number of axial half waves along the length, then $m = 1$ and n is determined from equation [10]. The factor 1.23 has to be adjusted so that n turns out as a whole number. Once n is determined then equation [9] will give the value of the buckling load for uniform loading. For nonuniform loading correction factors can be applied in accordance with a recent paper.⁸

IV. Buckling or yield

It is clear from Schuman's experiments² that both buckling and yield collapse can occur. The main problem is to be able to predict which type will take place. Once buckling or collapse has commenced the plastic deformation will take place in that particular pattern into which the failure has started. It will now be shown how equation [8] and [9] can be employed to determine whether a collapse or buckling will take place. Although there were some gross assumptions involved in the derivation of equation [8] the main item to be recognized is that the pressure for this type of yield is proportional to h/a and dependent on $\nu, \ell/a$. On the other hand the buckling pressure is critically dependent on $n, h/a$ and h^2/a^2 as well as $\nu, \ell/a$.

It should be made clear at this point that equation [8] and [9] are not to be used to approximate any of the dynamical parameters of the shell; they are to be used only to determine which type of failure

will start. Once this is known then the plastic analysis as given in a previous reference¹ will be employed to determine the plastic deflections and impulse values. Assuming that

$$E \approx 1000 \sigma_0, \beta = 2, \alpha = \frac{1}{2}$$

it was found that shell buckling or yield could be predicted by the equations in the previous section by employing the following criterion:

If the buckling load is less than the yield load the shell should buckle; if the yield load is less than the buckling then the shell should collapse.

Due to lack of experimental evidence on the load distribution the parameters β and α are questionable. Perhaps when more information is available about the load distribution more accurate computations can be performed. However our present calculations do indicate that the simplified equations presented above describe the physical phenomenon and enable prediction of the type of failure that will occur in a given cylindrical shell.

To illustrate the procedure for determining whether collapse or buckling failure will occur, consider several cylindrical shells that were tested.

1. Consider a steel shell with radius of 1.5", length 11.62", thickness .019" subjected to a lateral blast which is 8' away. The experiment showed that this shell formed a collapse hinge.

Using an $E = 1000 \sigma_0$, $\beta = 2$, $\alpha = \frac{1}{2}$, $\nu = .3$ the collapse load according to [8] is

$$(p_0)_c \approx .0013 \sigma_0$$

If the shell would buckle [10] predicts that $n = 3$. Then equation [9] shows that the uniform buckling load for this n is

$$(q_{cr})_b \approx .0021 \sigma_0$$

and using the nonuniform pressure correction⁸ it is seen that this value of $.0021 \sigma_0$ will be somewhat higher, possible as much as 50% greater. Thus for this shell $(p_0)_c < (q_{cr})_b$ so that

the shell can be expected to fail by collapse.

2. Consider next an aluminum shell of radius 1.5", length 6", thickness .006" subjected to a lateral blast which is 15' away. The experiment showed that this shell buckled with 6 lobes around the periphery and a half wave along the length. Using an $E = 1000 \sigma_0$, $\beta = 2$, $\alpha = \frac{1}{2}$, $\nu = .3$, the yield load would be

$$(p_0)_c \approx .0014 \sigma_0$$

Under buckling [10] predicts $n = 6$. Equation [9] shows that the uniform buckling pressure will be

$$(q_{cr})_b \approx .00024 \sigma_0$$

The correction for nonuniform loading could possible raise this value to $.00036 \sigma_0$. Thus for this shell $(q_{cr})_b < (p_0)_c$ so that the shell can be expected to buckle.

V. Post failure collapse and buckling

A. Collapse

It has been found¹ that the relation between the total impulse applied to the shell and the work done on the shell can be written as

$$I_t = \int_A \sqrt{V \frac{2\rho h}{\int_A g^2(x,y) dA}} g(x,y) dA \quad [11]$$

where $g(x,y)$ is the spatial distribution of the impulse, ρ is the mass density of the shell material, h is the shell thickness, and V is the work done on the shell in deforming it plastically. The integral is taken over the area, A , of the shell. By a systematic simplification it has been shown that V can be written as

$$V \approx \frac{2\sigma_0 h w_0 l}{\sqrt{3}} \int_0^1 \int_0^{2\pi} \bar{f}(x',\phi) d\phi dx' \quad [12]$$

where σ_0 is the yield stress in pure tension, w_0 is the maximum deflection, h is the thickness, l is the length and $\bar{f}(x',\phi)$ is the spatial distribution of the deflection, i.e.

$$w = w_0 \bar{f}(x',\phi)$$

The assumptions under which [12] was derived are

1. The shell is made of a perfectly plastic material
2. The radius of the shell is considerably smaller than the length ($a/l \ll 1$)
3. The deflection of the shell is much smaller than the radius ($w_0/a \ll 1$)
4. $w_0/\sqrt{3} \gg \epsilon_0 a/2$ where ϵ_0 is the yield strain

For details see Reference 1

The deflection pattern for collapse is shown in Figure 4 and can be written analytically as follows:

$$w(x,\phi) = a \cos \phi - \sqrt{a^2 - \frac{d_0^2}{4} \left[d_0 - \frac{d_0}{x_2} x \right]^2} \quad [13]$$

Letting $x' = x/l$

$$\begin{aligned} w(x,\phi) &= a \cos \phi - \sqrt{a^2 - \frac{d_0^2}{4} [1 - 2x']^2} \quad \text{for } 0 < x' < \frac{1}{2} \\ &= a \cos \phi - \sqrt{a^2 - \frac{d_0^2}{4} [1 + 2x']^2} \quad \text{for } -\frac{1}{2} < x' < 0 \end{aligned} \quad [14]$$

where d_0 is the width of the hinge line as shown in Figure 4. Using these deformation expressions and [12], the work done on the shell in deforming it plastically can be written as

$$V = \frac{2\sigma_0 h l}{\sqrt{3}} \left\{ \int_{-\frac{1}{2}}^0 \int_{-\phi_1(x')}^{\phi_1(x')} \left[a \cos \phi - \sqrt{a^2 - \frac{d_0^2}{4} [1+2x']^2} \right] d\phi dx' + \int_0^{\frac{1}{2}} \int_{-\phi_1(x')}^{\phi_1(x')} \left[a \cos \phi - \sqrt{a^2 - \frac{d_0^2}{4} [1-2x']^2} \right] d\phi dx' \right\} \quad [15]$$

where

$$\begin{aligned} \phi_1 &= \sin^{-1} \frac{d_0(1-2x')}{2a} \quad \text{for } 0 < x' < \frac{1}{2} \\ \phi &= \sin^{-1} \frac{d_0(1+2x')}{2a} \quad \text{for } -\frac{1}{2} < x' < 0 \end{aligned} \quad [16]$$

After some mathematical manipulation and substitution of

$$y = \frac{d_0}{2a} [1+2x'] \quad , \quad y' = \frac{d_0}{2a} [1-2x'] \quad [17]$$

it is found that V can be written

$$V = \frac{2\sigma_0 h l}{\sqrt{3}} \frac{4a}{2\frac{d_0}{2a}} \int_0^{d_0/2a} (y - \sqrt{1-y^2} \sin^{-1} y) dy \quad [18]$$

or finally

$$V = \frac{2\sigma_0 h l d}{\sqrt{3}} \frac{1}{\frac{d_0}{d}} \left[\frac{3}{4} \left(\frac{d_0}{d} \right)^2 - \frac{\bar{\phi}^2}{4} - \frac{\bar{\phi}}{2} \frac{d_0}{d} \sqrt{1 - \left(\frac{d_0}{d} \right)^2} \right] \quad [19]$$

$$\text{where } \bar{\phi} = \sin^{-1} d_0/d \quad d = 2a$$

Now using the impulse equation [11] and assuming that

$$g(x, y) \equiv g(x, \phi) = e^{-\beta \phi}$$

The relation between the impulse and the deformation can be written as

$$I_t = 2hld \sqrt{\kappa} \sqrt{\frac{\sigma_0 p}{\sqrt{3}}} \quad [20]$$

$$\text{where } \kappa = \frac{1}{\frac{d_0}{d}} \left[\frac{3}{4} \left(\frac{d_0}{d} \right)^2 - \frac{\bar{\phi}^2}{4} - \frac{\bar{\phi}}{2} \frac{d_0}{d} \sqrt{1 - \left(\frac{d_0}{d} \right)^2} \right]$$

The deflection is actually described by d_0/d . A plot of $\sqrt{\kappa}$ as a function of d_0/d is given in Fig. 5.

Some calculations were run on several of the tested shells which failed by collapse and these computations with the experimental results are given below. A given value of deflection corresponding to a given d_0/d was measured from the tests and the incident and reflected impulse per unit area corresponding to this d_0/d were also measured. The theory (eq. [20] above) predicts the impulse which will produce a given d_0/d . Unfortunately the exact value of the experimental impulse was not given but the incident impulse*per unit

*The incident impulse is the measured impulse without an obstruction such as the shell. The reflected impulse is the impulse that reflects off of a large rigid plane.

area $(\bar{I}_e)_i$; and the reflected impulse per unit area $(\bar{I}_e)_r$ were the parameters that were measured. The actual impulse applied to the shell will be somewhere between these values of $(\bar{I}_e)_i$ and $(\bar{I}_e)_r$.

Assuming that the measured values would correspond to maximum values on the shell and assuming an $e^{-\beta\phi}$ distribution of the impulse on the shell it is seen that the total impulse would be

$$(I_t)_e = 2 \int_0^l \int_0^\pi (\bar{I}_e) e^{-\beta\phi} \sin\phi d\phi dx \quad [21]$$

$$\text{So } (\bar{I})_e \approx 2 \frac{(I_t)_e}{dl}$$

So the theoretical value to compare with the measurements is

$$\bar{I} = 2 \frac{I_t}{dl} = 4h\sqrt{k} \sqrt{\frac{\sigma_0 \rho}{\sqrt{3}}} \quad [22]$$

A value of $\sigma_0 \approx 50,000 \text{ psi}$ was assumed for the steel shells that were tested

Example 1

$$\begin{aligned} d &= 3", \quad l = 6", \quad h = .019" \\ \text{For } d_0/d &\approx 1 \quad \sqrt{k} \approx .36 \text{ from Fig. 5} \\ \text{So } \bar{I} &\approx 123 \text{ psi millisecc.} \end{aligned}$$

The measured values which gave the shell a deformation in which $d_0/d \approx 1$ were

$$(\bar{I}_e)_i = 89 \text{ psi millisecc.}, \quad (\bar{I}_e)_r = 299 \text{ psi millisecc.}$$

Example 2

$$\begin{aligned} d &= 3", \quad l = 8.62", \quad h = .019" \\ \text{For } d_0/d &\approx .8, \quad \sqrt{k} \approx .24 \\ \bar{I} &\approx 82 \text{ psi millisecc.} \end{aligned}$$

The measured values were

$$(\bar{I}_e)_i = 15.5 \text{ psi millisecc.}, \quad (\bar{I}_e)_r = 69.5$$

Example 3

$$\begin{aligned} d &= 3", \quad l = 8.62", \quad h = .019" \\ \text{For } d_0/d &\approx .75, \quad \sqrt{k} \approx .21 \\ \bar{I} &= 71.5 \text{ psi millisecc.} \end{aligned}$$

The measured values were

$$(\bar{I}_e)_i = 48, \quad (\bar{I}_e)_r = 160$$

Example 4

$$\begin{aligned} d &= 3", \quad l = 11.62", \quad h = .019" \\ \text{For } d_0/d &\approx .75 \quad \sqrt{k} \approx .21 \quad \bar{I} \approx 71.5 \text{ psi millisecc.} \end{aligned}$$

The measured values were

$$(\bar{I}_e)_i = 14.5, \quad (\bar{I}_e)_r = 56.1$$

Example 5 $d = 3''$, $l = 11.62''$, $h = .019''$
 For $d_0/d \approx .75$, $\sqrt{K} \approx .21$, $\bar{I} \approx 71.5$

The measured values were

$$(\bar{I}_e)_i = 25 \quad (\bar{I}_e)_r = 83$$

Example 6 $d = 3''$, $l = 18''$, $h = .019''$
 For $d_0/d \approx 1$, $\bar{I} \approx 123$

The measured values were

$$(\bar{I}_e)_i = 68 \quad (\bar{I}_e)_r = 190$$

Example 7 $d = 6''$, $l = 18''$, $h = .019''$
 For $d_0/d \approx .75$, $\bar{I} \approx 71.5$

The measured values were

$$(\bar{I}_e)_i = 22 \quad (\bar{I}_e)_r = 67$$

Example 8 $d = 6''$, $l = 17.5''$, $h = .035''$
 For $d_0/d \approx .75$, $\bar{I} \approx 143$

The measured values were

$$(\bar{I}_e)_i = 64 \quad (\bar{I}_e)_r = 200$$

The different impulse values arose from various explosive charge weights and distances of explosion from the shell.

The comparisons between the theoretical predictions and experimental results show that the simplified equations predict the correct order of magnitude for the impulse which will result in a given deflection. When more exact experimental values are available for the applied impulse more accurate computations using the more accurate general work expression of Reference 1 can be made.

B. Buckling

For the post failure buckling region the circumferential parameter n takes on great importance and the simplification given by equation [12] cannot be employed. Instead, the plastic work has to be computed from the more general integral expressions given in Reference 1. We use equation [40] in the "Errata and Addendum of Reference 1 and assume a post failure deflection pattern of the form

$$\begin{aligned} \bar{f}(x, \varphi) &= \sin \pi x' e^{-k\varphi} \cos n\varphi \quad \text{for } 0 < \varphi < \pi \\ &= \sin \pi x' e^{-k(2\pi-\varphi)} \cos n(2\pi-\varphi) \quad \text{for } \pi < \varphi < 2\pi \end{aligned}$$

[23]

and an impulse distribution the same as before, i.e.

$$I = (\bar{I}_e) e^{-\beta \phi} \quad (\beta = 2)$$

The shell used was made of aluminum and was in diameter, 9" long, and .006" thick. A yield stress of 15,000 psi was assumed. Numerical integration of equation [40] of Reference 1 was performed assuming a perfectly plastic material and $k = \frac{1}{4}$, $n = 5$. The value of $n = 5$ was obtained from equation [10] and compared well with the experimental result. The calculated peak impulse per unit area to produce $w_0/a \approx .5$ is 21 psi milliseconds. The experiments showed that the blast load which produced an incident impulse of 21.1 psi milliseconds and reflected impulse of 46.8 gave $w_0/a \approx 0.5$.

VI. Conclusions

One cannot apriori assume the type of deformation into which a shell will deform under blast load unless some pre-failure computations are made to determine whether the shell will collapse or buckle. Schuman's experiments² point out that these two types of patterns can exist. The computations and experimental comparisons given in this report indicate that

1. It can be predicted whether a shell will fail in buckling or collapse by use of equation [8] and [9] of this report.
2. Once the failure type is known the order of magnitude of the impulse and energy to produce a given plastic deformation can be computed for side-on lateral loads by assuming a collapse pattern of the form of equation [13] for collapse failure and a buckled pattern of the form [23] for post buckling behavior in the plastic region.

The equations given in Reference 1 have been programmed for the BRL computer. This will enable future computations with more complicated deflection patterns.

REFERENCES

1. J. E. Greenspon, "Elastic and Plastic Behavior of Cylindrical Shells Under Dynamic Loads Based on Energy Criteria," J G Engineering Research Associates, " Contract No. DA 36-034-ORD-3081 RD, Tech. Rep. No. 3, Feb., 1963.)Under contract with Ballistic Research Laboratories, Aberdeen Proving Ground)
2. W. J. Schuman, Jr., "The Response of Cylindrical Shells to External Blast Loading," Ballistic Research Laboratories, Aberdeen Proving Ground, Memorandum Report No. 1461, March, 1963.
3. W. Flugge, "Stresses in Shells," Springer Verlag, 1962, pp. 108-110, 131.
4. V. V. Novozhilov, "The Theory of Thin Shells," Translated by P. G. Lowe, edited by J. R. M. Radok, P. Noordhoff Ltd., Groningen, The Netherlands, 1959, p. 99, 169.
5. S. Timoshenko, "Theory of Elastic Stability," McGraw Hill Book Company, 1936, First Edition, Eighth Impression.
6. Ibid, p. 450.
7. T. E. Reynolds, "Inelastic Lobar Buckling of Cylindrical Shells Under External Hydrostatic Pressure," David Taylor Model Basin Report 1392, August, 1960.
8. B. O. Almroth, "Buckling of a Cylindrical Shell Subjected to Nonuniform External Pressure," Journal of Applied Mechanics, Dec., 1962, p. 675.



Fig. 1a. Buckling

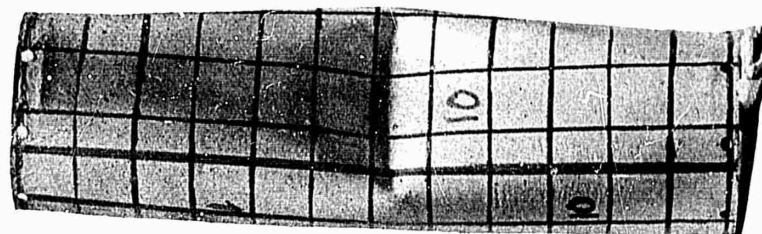


Fig. 1b. Collapse

Fig. 1. Types of Failure (from Schuman's experiments, see Ref. 2)

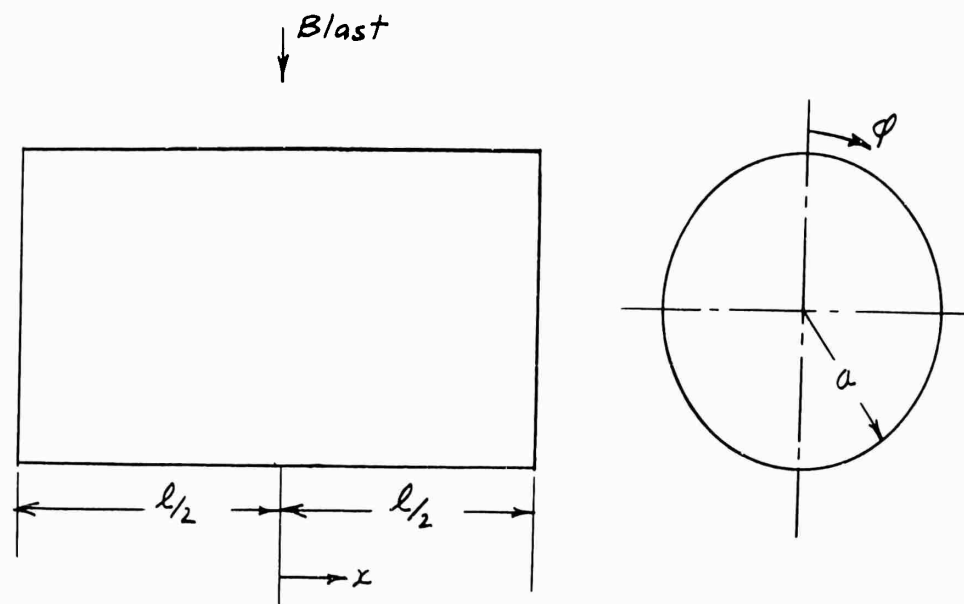


Fig. 2 Origin of Coordinates

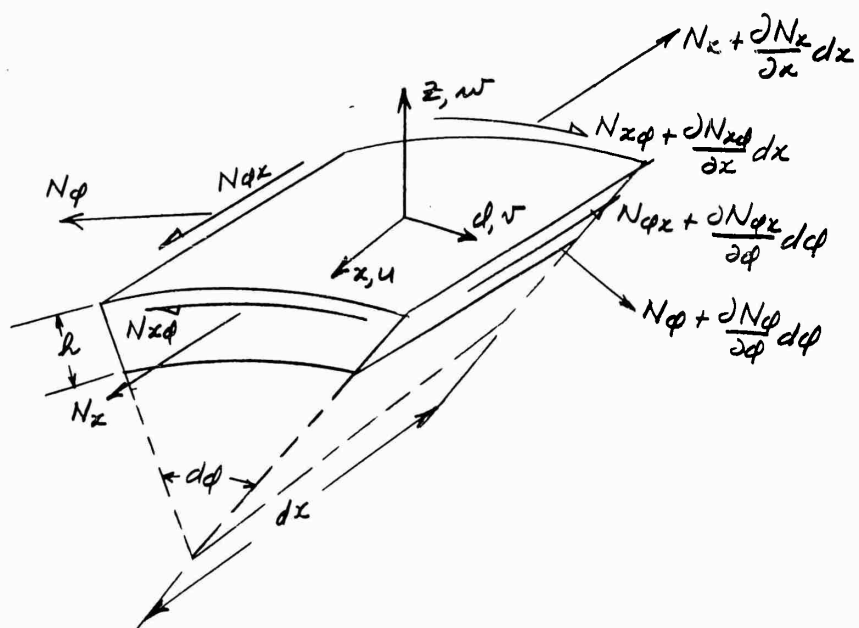


Fig. 3 Shell Element

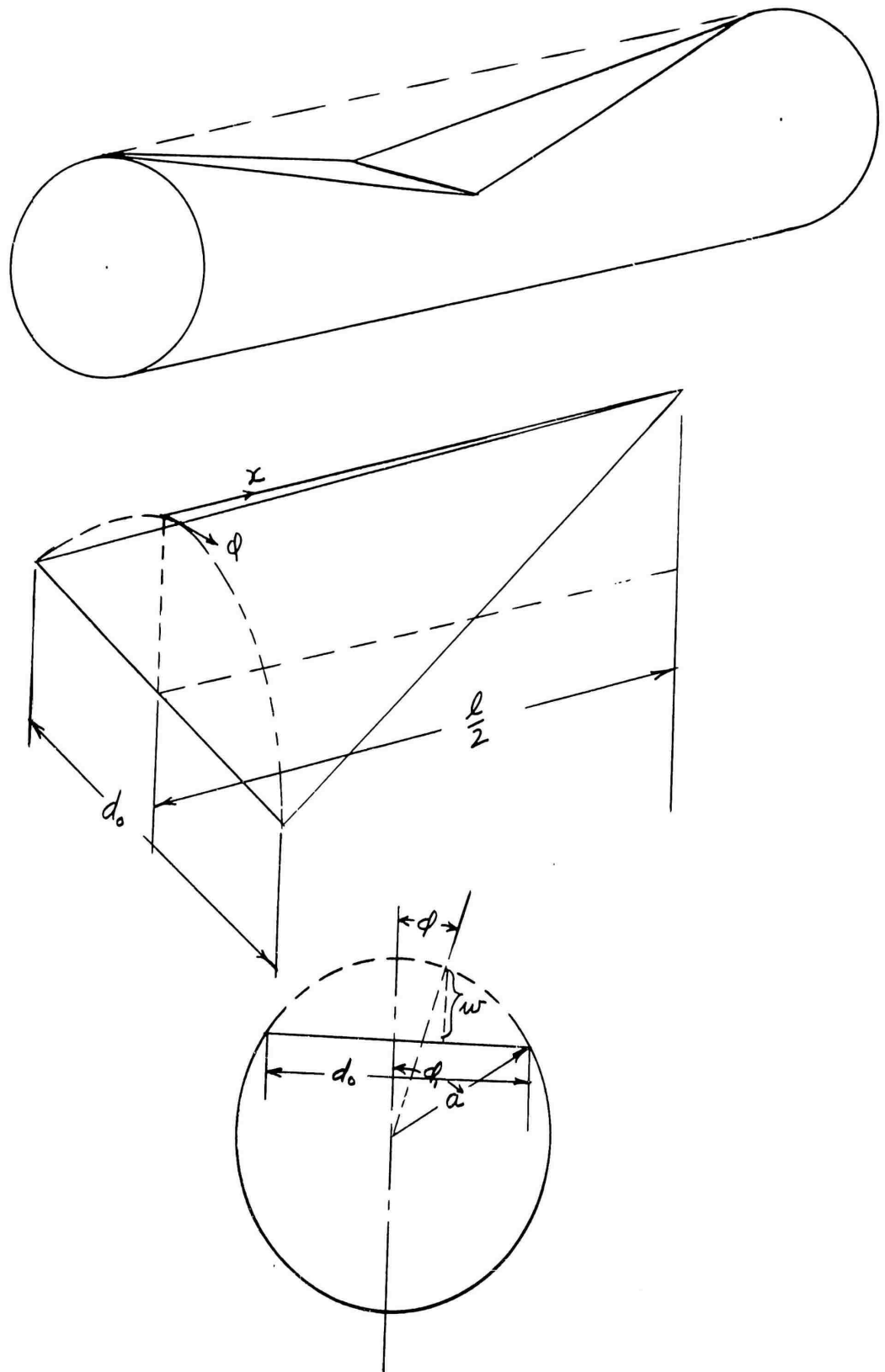


Fig. 4 Collapse Pattern

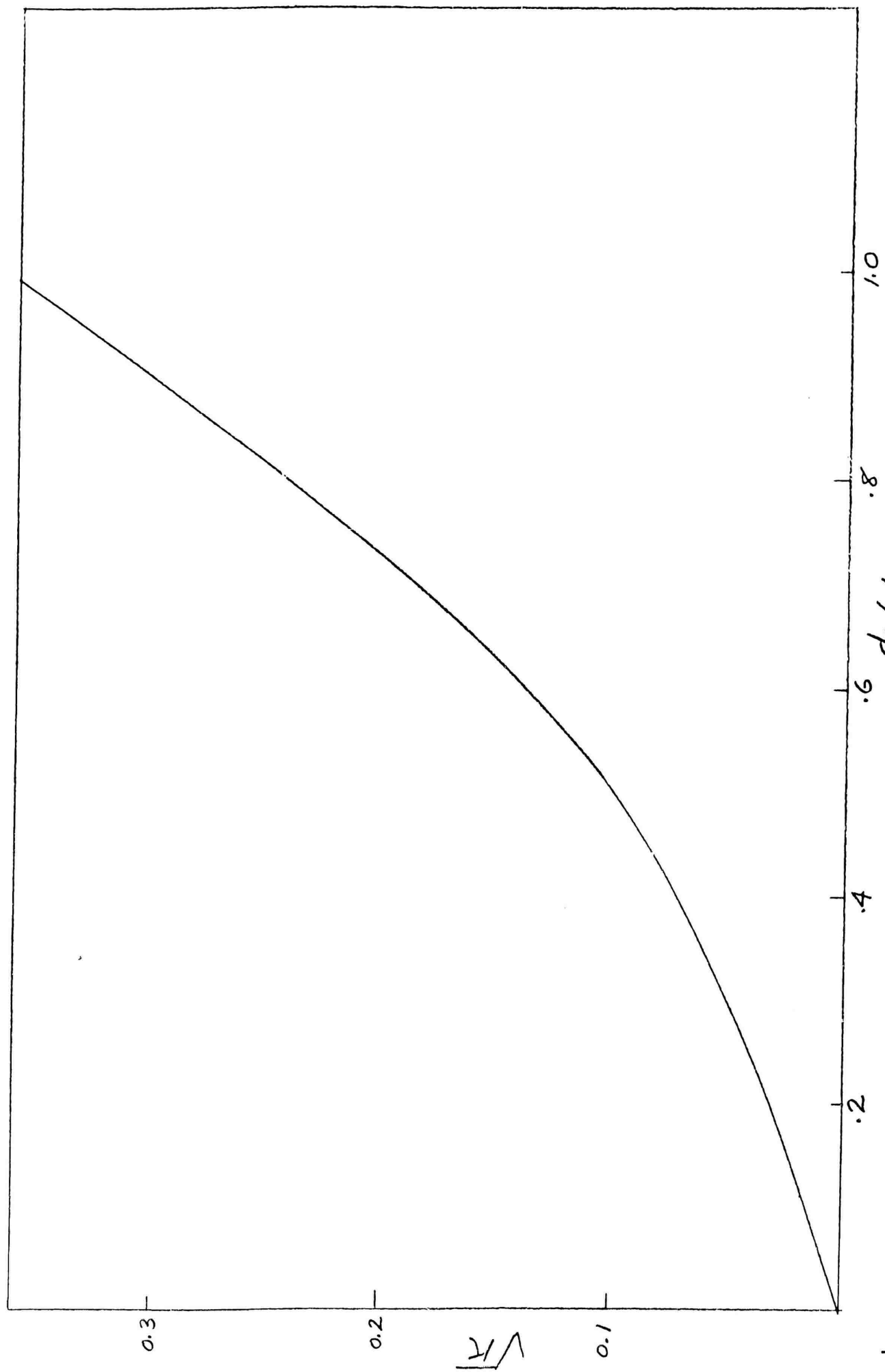


Fig. 5 Plot of \sqrt{R} as a Function of d_o/d